Dynamic dependence of interaction potentials for keV atoms at metal surfaces

A. Schüller, G. Adamov, S. Wethekam, K. Maass, A. Mertens, and H. Winter*

Institut für Physik, Humboldt Universität zu Berlin, Brook-Taylor-Strasse 6, D-12489 Berlin, Germany

(Received 8 March 2004; published 28 May 2004)

He and N atoms are scattered with keV energies under a grazing angle of incidence from clean and flat Ag(111) and Al(111) surfaces. For incidence along low index crystallographic directions in the surface plane, atomic projectiles are steered by rows of atoms ("axial surface channeling") giving rise to characteristic rainbows in their angular distribution. From the analysis of this effect we derive effective scattering potentials which reveal pronounced dynamical effects. We attribute our observation to the embedding energy for penetration of atoms in the electron gas of a metal.

In atomic collisions, the interaction potentials play a crucial role in the description and understanding of scattering processes. As a consequence, the analysis of experimental data in terms of scattering potentials is a key issue in collision physics. For example, atomic collisions in solids describing a variety of phenomena as angular straggling, projectile ranges in matter, energy dissipation, ion implantation, ion backscattering, or channeling are directly based on interaction potentials [1].

With respect to this Rapid Communication, we mention low and medium energy ion scattering which has developed in recent years to a powerful real-space method for the precise determination of the geometrical structure of crystal surfaces [2,3]. Here the sequence of scattering events involving target atoms in the first few surface layers are analyzed in terms of focusing and blocking effects that give rise to enhanced or reduced intensities for large angle scattering (backscattering) of fast atomic projectiles. In order to deduce from data the arrangement of atoms in the topmost surface layers, interatomic potentials with electronic screening described in the Thomas-Fermi approximation are generally used. Coulomb potentials with "universal screening" as proposed by Ziegler, Biersack, and Littmark (ZBL) [1] or with screening as given by O'Connor and Biersack (OCB) [4] provide in most cases a good basis for the structural analysis of crystalline surfaces and ultrathin films.

When particles are scattered for different impact parameters under comparable angles, i.e., for extrema of the deflection function (scattering angle vs impact parameter), so-called "rainbows" are identified in the angular distributions [5]. Rainbow effects observed in low energy scattering of atoms and ions from crystalline surfaces are reviewed by Kleyn and Horn [6].

An important aspect of rainbow effects for scattering of atomic projectiles from surfaces is the close correspondence of typical features of rainbows, primarily the scattering angle for an enhanced intensity of scattered projectiles ("rainbow angle"), to effective interaction potentials. This was considered in large angle scattering of hyperthermal Na$^+$ ions (en-

ergies up to some 100 eV) from Cu surfaces [7,8] where pair potentials consistent with Hartree-Fock calculations and an attractive image charge potential were derived.

In this Rapid Communication we report on studies where rainbow scattering of fast atomic projectiles under surface channeling is exploited to deduce interaction potentials. Atomic projectiles with energies up to some 10 keV are scattered under a grazing angle of incidence from Ag(111) and Al(111) surfaces. In this regime of atomic collisions with solids, scattering proceeds in the regime of "surface channeling" [9,10] where projectiles are steered in a sequence of small angle scattering from planes ("planar channeling") or strings ("axial channeling") of atoms of a regular crystal lattice. The description of trajectories for scattering under channeling conditions is well approximated by continuum interaction potentials obtained from averaging over atomic planes or strings of a crystal [9–11]. Interaction potentials for atomic projectiles at a crystal surface show planar and axial symmetry with respect to atomic planes and strings, respectively. Defined trajectories for ensembles of projectiles, compared to large angle scattering, lead to a simpler and more direct interpretation of data [12]. In order to avoid effects of the image charge on projectile trajectories, neutral atoms are selected on the incoming and outgoing path [13].

In the left panel of Fig. 1 we have sketched equipotential lines for He atoms scattered from ⟨110⟩ strings formed by Ag atoms at the topmost layer of Ag(111) surface. Note that for grazing scattering, i.e., axial surface channeling, and neglect of projectile energy loss, the energies of motion along and normal to strings are conserved, so that atoms move with constant energy parallel to strings. The scattering process with the solid is governed by the normal motion with energy E_z. We show projections of trajectories into a plane normal to atomic strings (xz plane) and equipotential curves with about sinusoidal shape. This results in extrema in the angular deflection giving rise to rainbow effects [6,12], i.e., enhanced intensities for projectiles scattered out of the plane of incidence by the "rainbow angle" Θ_{rb}.

In the right panel of Fig. 1 we present a contour plot of an experimental angular distribution for 2.8 keV He atoms scattered under a grazing angle of incidence $\Phi_{in}=1.2°$ along the ⟨110⟩ direction in the (111) plane of a clean and flat monocrystalline Ag sample. The experiments were performed with

---

*Author to whom correspondence should be addressed. Electronic address: winter@physik.hu-berlin.de
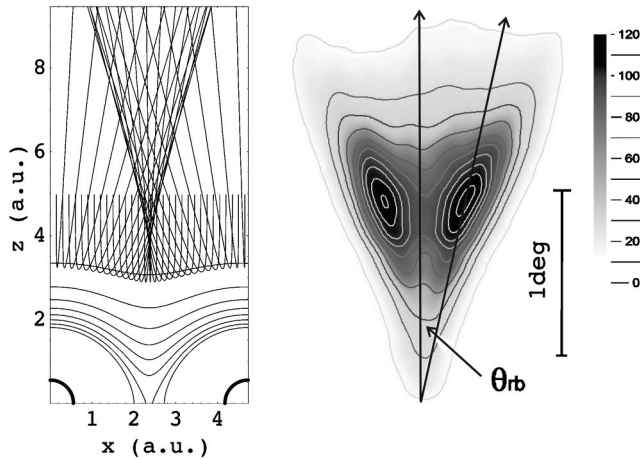
FIG. 1. Left panel: Projections of classical trajectories in plane normal to ⟨110⟩ axial channels for He atoms scattered with E_z =1.2 eV from Ag(111). Equipotential curves in 1 eV intervals are shown (from 1 to 8 eV). Right panel: Contour plot of experimental angular distribution for 2.8 keV He atoms scattered under Φ_{in} =1.2° (E_z=1.2 eV).

well collimated beams of fast atoms at a pressure of some 10^{-11} mbar. Angular distributions for scattered projectiles were recorded by means of a position-sensitive channelplate detector [14]. The angular positions of the two peaks, ascribed to rainbow scattering, provide the rainbow angle Θ_{rb}. This angle is compared with trajectory calculations based on pair potentials averaged along atomic strings (continuum potentials). For random azimuthal orientation of the target surface, we find well-defined single peaks which serve as reference for Φ_{in}.

In Fig. 2 we show the rainbow angle Θ_{rb} for He atoms scattered from a Ag(111) surface as a function of energy E_z for the motion normal to the surface. Since for channeling $E_z=E\sin^2\Phi_{in}$ holds, E_z can be tuned for a given projectile
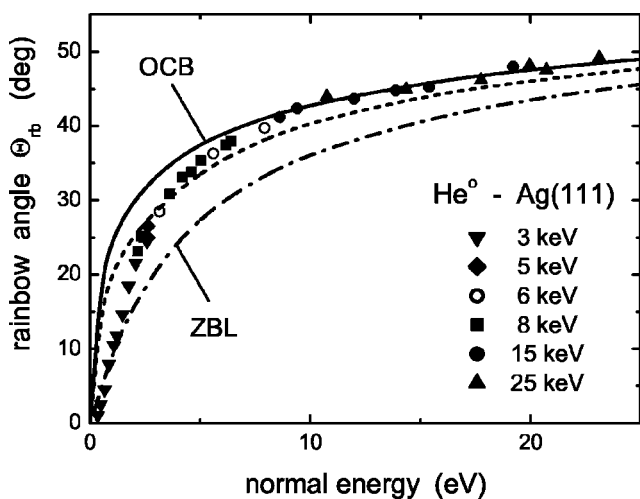

FIG. 2. Rainbow angle Θ_{rb} as a function of normal energy E_z for He atoms scattered from Ag(111) with energies 3, 5, 6, 8, 15, and 25 keV. Solid curve, classical trajectory calculations using OCB screening; dashed curve, OCB potential and full cohesive function (f=1); and dashed-dotted curve, ZBL-screening.
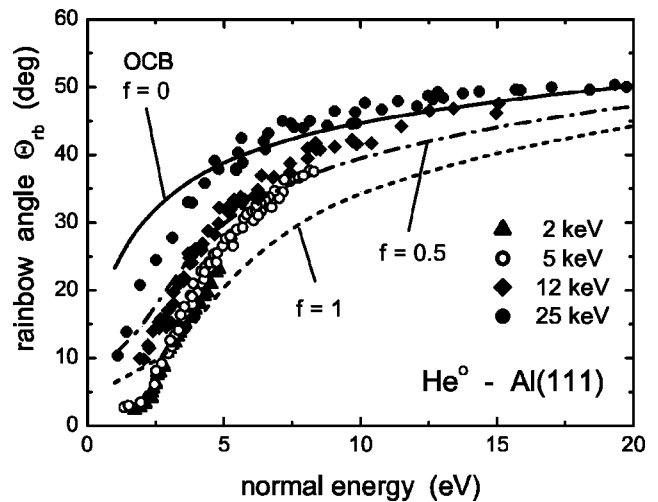

FIG. 3. Rainbow angle Θ_{rb} as a function of normal energy E_z for He atoms scattered from Al(111) with energies 2, 5, 12, and 25 keV. Solid curve, classical trajectory calculations using OCB screening (f=0); dashed-dotted curve, f=0.5; and dashed curve, inclusion of full cohesive function (f=1). For details see text.

energy E by the grazing angle of incidence Φ_{in}. In accordance with the potential curves shown in Fig. 1, the corrugation increases with E_z and results in a monotonic enhancement of Θ_{rb}. The rainbow angle is closely related to the geometry of equipotential surfaces so that (averaged) interatomic pair potentials can be directly probed. We present results from trajectory calculations based on classical mechanics using ZBL (dashed-dotted curve) and OCB (solid curve) pair potentials averaged over atomic strings. Discrete atom-atom potentials as well as thermal vibrations of lattice atoms are neglected here because continuum potentials are considered as good approximation in the channeling regime [9] and lattice vibrations will affect the angular spread for scattered projectiles but to a lesser extent angular peak shifts [15]. For OCB potentials we find good agreement for normal energies $E_z\geq5$ eV, ZBL potentials give (aside from low E_z) smaller rainbow angles, i.e., the latter potentials are too repulsive (see also, e.g., Pfandzelter *et al.* [16]). For Ne and Ar we observe similar results, in particular, no dependence on projectile energy (velocity) is found within the scatter of data. The dashed curve represents calculations with OCB potentials under incorporation of additional contributions from embedding of projectiles in the electron gas at the surface (see discussion below).

In Figs. 3 and 4 we display results from studies with He and N atoms scattered under grazing incidence from an Al(111) surface. The dependence of Θ_{rb} on E_z is different from that observed for Ag(111). A striking feature is a pronounced dependence of the data for Ag(111) on projectile energy (velocity), clearly different for He and N projectiles. In reference to calculations based on OCB potentials (solid curves with f=0, see below), the data for He atoms can be characterized by a pronounced decrease of Θ_{rb} with decreasing projectile energy at constant E_z. The data for N atoms shows the opposite trend with a substantial increase of Θ_{rb} towards small energies E. Such pronounced dynamic effects for the scattering process are somewhat surprising, since for
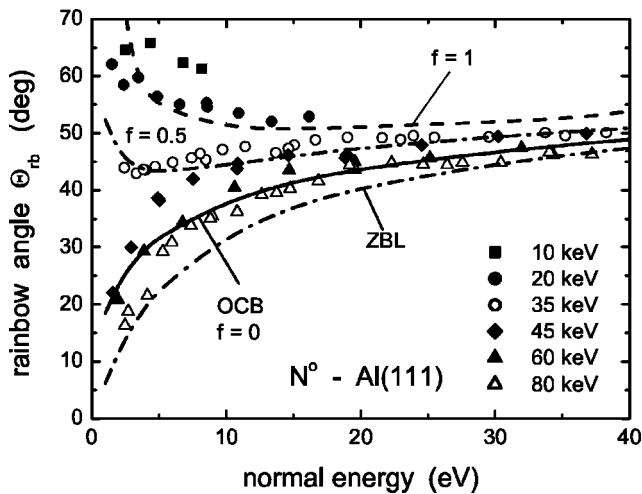
FIG. 4. Rainbow angle Θ_{rb} as a function of normal energy E_z for N atoms scattered from Al(111) with energies 10, 20, 35, 45, 60, and 80 keV. Classical trajectory calculations using OCB screening; solid curve, $f=0$; dashed-dotted curve, $f=0.5$; and dashed curve, $f=1$. For details see text.

FIG. 5. Rainbow angle Θ_{rb} as a function of projectile energy for He atoms scattered from Al(111) with a fixed normal energy E_z =4.2 eV. Solid curve, classical trajectory calculations using OCB screening and cohesive function with energy dependent factor f; dotted line, OCB screening only ($f=0$); and dashed line, inclusion of full cohesive function ($f=1$).

projectile energies below some 10 keV (projectile velocities below some 0.1 a.u.) screened Coulomb potentials are not expected to show a dynamic dependence. This holds also for retardation effects present for dielectric response phenomena [17].

In exploring the origin of the observed effects, we mention the density of conduction electrons, which is about a factor of 3 higher for Al as compared to Ag. Then the scattering potential might be modified by contributions from interactions of projectile atoms with the electron gas of the metal surface. Al has a relatively high bulk electron density of $n_e=0.026$ a.u.$^{-3}$ which decays about exponentially in the selvedge of the surface. For atoms embedded in an electron gas of given density n_e, screening effects modify their electronic structure. The resulting embedding energy represents the atomic binding energy as a function of n_e (cohesive function) [18]. Local density approximation (LDA) calculations by Puska and Nieminen [19] reveal for noble gas atoms repulsive potentials (positive cohesive functions), whereas for atoms forming negative ions within an electron gas attractive potentials are found. Cohesive functions (cohesive energies) are closely related to bond lengths and chemisorption at metal surfaces [20].

Such potentials added to the (averaged) interatomic pair potentials provide a consistent interpretation of the experiments. On a qualitative level, a (planar) repulsive embedding potential results in less corrugated equipotential curves for given energies E_z and smaller rainbow angles. For reactive atoms one expects the opposite behavior; in particular, the large Θ_{rb} observed for N atoms with small normal energies can only be understood by an additional attractive potential. Both scenarios explain the experimental findings.

For a quantitative analysis, we made use of cohesive functions for He and N as calculated by Puska [18,19], with the electron density in front of an Al(111) surface adjusted to pseudopotential calculations [21]. In trajectory calculations we added these potentials to the pair potentials with OCB
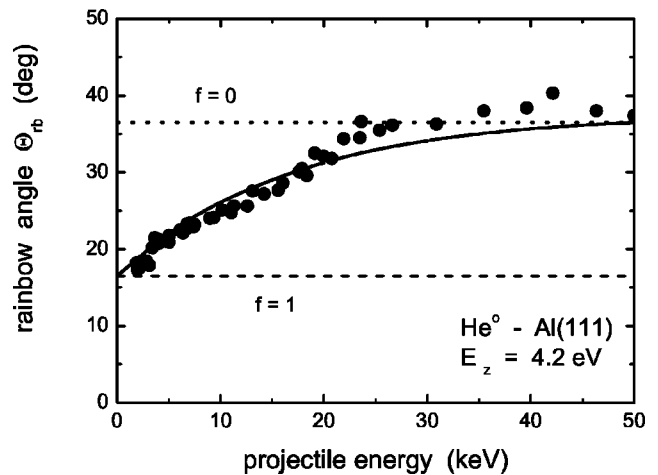
screening. In a simple approach, dynamic effects for the cohesive function were taken into account by a factor f ($f=1$, full cohesive function; $f=0$, no cohesive function). Our calculations for the two limiting cases ($f=0, f=1$) and $f=0.5$ give an idea on the dynamic properties of the cohesive function (cf. Figs. 3 and 4).

A more detailed investigation of dynamic effects is performed with He atoms scattered from Al(111), where—for a controlled variation of the projectile energy—$E_z=4.2$ eV is kept constant by an adjustment of the angle of incidence Φ_{in}. The data in Fig. 5 reveal the expected increase of the rainbow angle Θ_{rb} with increasing projectile energy. The dynamic limits are the full cohesive function at rest (dashed line, $f=1$) and at high energies by averaged pair potentials (OCB screening: dotted line, $f=0$). We find a fair description for the dynamic effects by the arbitrarily chosen analytical expression $f(E)=\exp(-cE)$ with $c_{He} \approx 1/15$ keV as a free parameter for the He–Al system. The dynamic effects for N–Al are described with $c_N \approx 1/55$ keV $\approx c_{He}4$ amu/14 amu. So our description of dynamic effects for the two cases scales with projectile energy per mass unit, i.e., velocity [22].

At present, we are not aware of calculations on cohesive functions taking into account dynamic effects. Thus a more detailed analysis of the observed effects is beyond the scope of the present paper. However, the comparison with dynamic effects present in dielectric response phenomena [17] indicates that those effects are more pronounced here. Screening effects on the energies of atoms embedded in an electron gas show a stronger dynamic dependence than long-range interactions.

In conclusion, by making use of specific features for grazing scattering of fast atoms from monocrystalline metal surfaces we exploit rainbow effects under axial surface channeling to deduce effective scattering potentials. For an Al(111) surface we observe pronounced dynamic effects which are attributed to contributions of the cohesive function, i.e., en-

ergies of atoms embedded in an electron gas. In accord with LDA calculations these potentials are repulsive for noble gas atoms (see data for He) and attractive for atoms reactive in the electron gas (see data for N). For Ag(111) the electron densities at the surface are clearly smaller so that these effects are strongly reduced (dashed curve in Fig. 2). To the best of our knowledge these contributions to the interaction potentials have not been considered so far in collisions of keV atoms and ions with solids and, in particular, solid surfaces. Our studies give clear evidence for the presence of such effects and have important consequences for the field of atomic collisions with solids.

At first, the description and analysis of binary atomic collisions with target atoms embedded in a metal has to take into account the additional potential owing to the penetration of projectiles into the electron gas of the metal. The corresponding potential energies up to some eV will affect small angle scattering, i.e., collisions with larger impact parameters. This modifies, in particular, trajectories of atomic projectiles scattered from metal surfaces at glancing angles and/or low energies.

Second, the pronounced dynamic effects observed here for the cohesive functions have to be analyzed from first principles for a detailed understanding of ion-solid interactions. Since the interactions take place in the selvedge of the surface, effects caused by gradients of electron densities have to be taken into account also. In this respect we hope that our work will stimulate theoretical calculations on this problem.

[1] J. F. Ziegler, J. P. Biersack, and U. Littmark, *The Stopping and Range of Ions in Solids* (Pergamnon Press, New York, 1985), Vol. 1.

[2] H. Niehus, W. Heiland, and E. Taglauer, Surf. Sci. Rep. **17**, 213 (1993).

[3] J. W. Rabalais, Science **250**, 521 (1990).

[4] D. J. O'Connor and J. P. Biersack, Nucl. Instrum. Methods Phys. Res. B **15**, 14 (1986).

[5] E. W. McDaniel, J. B. A. Mitchell, and M. E. Rudd, *Atomic Collisions* (Wiley, New York, 1993).

[6] A. W. Kleyn and T. C. M. Horn, Phys. Rep. **199**, 191 (1991).

[7] D. L. Adler and B. H. Cooper, Phys. Rev. B **43**, 3876 (1991).

[8] C. A. DiRubio, R. L. McEachern, J. G. McLean, and B. H. Cooper, Phys. Rev. B **54**, 8862 (1996).

[9] D. Gemmell, Rev. Mod. Phys. **46**, 129 (1974).

[10] H. Winter, Phys. Rep. **367**, 387 (2002).

[11] C. Erginsoy, Phys. Rev. Lett. **15**, 360 (1965).

[12] D. M. Danailov, R. Pfandzelter, T. Igel, H. Winter, and K. Gärtner, Appl. Surf. Sci. **171**, 113 (2001).

[13] H. Winter, J. Phys.: Condens. Matter **8**, 10149 (1996).

[14] Roentdek GmbH, Kelkheim-Ruppertshain, Germany.

[15] R. Pfandzelter, Phys. Rev. B **57**, 15496 (1998).

[16] R. Pfandzelter, F. Stölzle, H. Sakai, and Y. H. Ohtsuki, Nucl. Instrum. Methods Phys. Res. B **83**, 469 (1993).

[17] P. M. Echenique, F. Flores, and R. H. Ritchie, *Solid State Physics* (Academic Press, New York, 1990), Vol. 43, p. 229.

[18] M. J. Puska, in *Springer Proceedings in Physics* (Springer, Berlin, 1990), Vol. 48, p. 134.

[19] M. J. Puska and R. M. Nieminen, Phys. Rev. B **43**, 12221 (1991).

[20] J. K. Nørskov, Rep. Prog. Phys. **53**, 1253 (1990).

[21] K. J. Bohnen (private communication).

[22] Observed dynamic effects scale with energy per mass unit (velocity), however, $f = \exp(-av)$ does not give satisfactory scaling in comparison to $f = \exp(-cE) = \exp(-bv^2)$; a, b, c = constants.